IOPscience iopscience.iop.org

Home Search Collections Journals About Contact us My IOPscience

Strong barrier effect on the conversion efficiency of solar cells with buried type-II quantum dots

This content has been downloaded from IOPscience. Please scroll down to see the full text.

2007 Semicond. Sci. Technol. 22 616

(http://iopscience.iop.org/0268-1242/22/6/006)

View the table of contents for this issue, or go to the journal homepage for more

Download details:

IP Address: 140.113.38.11
This content was downloaded on 26/04/2014 at 05:38

Please note that terms and conditions apply.

IOP PUBLISHING SEMICONDUCTOR SCIENCE AND TECHNOLOGY

Semicond. Sci. Technol. **22** (2007) 616–623 doi:10.1088/0268-1242/22/6/006

Strong barrier effect on the conversion efficiency of solar cells with buried type-II quantum dots

A M Kechiantz[1,2], K W Sun[1], H M Kechiyants[2] and L M Kocharyan[3]

[1] Department of Applied Chemistry and Institute of Molecular Science, National Chiao Tung University, Hsinchu, Taiwan
[2] Scientific Research Division, State Engineering University of Armenia, Yerevan, Armenia
[3] Department of Physics, State University of Armenia, Yerevan, Armenia

E-mail: MRS_Armenia@yahoo.com, arakech@mail.nctu.edu.tw and kwsun@mail.nctu.edu.tw

Received 21 January 2007, in final form 2 April 2007
Published 4 May 2007
Online at stacks.iop.org/SST/22/616

Abstract
A model of a quantum dot (QD) buried solar cell is described. The cell takes advantage of the generation of an additional photocurrent by a two-photon excitation of electrons from the valence band into the conduction band via the confined (intermediate) state. Since the intermediate states are active recombination centres suppressing the open-circuit voltage and the conversion efficiency either by increasing the dark-current or by arresting the quasi-Fermi level of mobile carriers, a barrier layer promoting the separation of the quasi-Fermi levels is built in around the QDs. Conditions for the separation of the quasi-Fermi levels and the activation of the two-photon generation of mobile carriers were found. Under these conditions the photocurrent and the conversion efficiency of the Ge QD buried Si solar cell exposed to concentrated sunlight must be approximately 25% larger than that of conventional Si solar cells.

List of symbols

α_C and α_V — absorption coefficients for the direct electron transitions from the confined state into the conduction band and from the valence band into the confined state within the Ge QDs, $\alpha_C = \beta_C(N_D - p_D)$ and $\alpha_V = \beta_V p_D$, $\alpha_C = \alpha_V \approx 10^3$ cm^{-1};

α_Γ — absorption coefficient for the direct electron transitions in the bulk Ge, $\alpha_\Gamma \approx \beta_\Gamma N_{C\Gamma}$, $\alpha_\Gamma \geqslant 5 \times 10^3$ cm^{-1};

β_C, β_V and β_Γ — relevant absorption cross-sections, $\beta_C \approx 8 \times 10^{-13}$ cm^2 [39], $\beta_V = 2 \times 10^{-13}$ cm^2 [26], $\beta_\Gamma \approx 2.5 \times 10^{-14}$ cm^2, $\beta_C = \beta_V \approx 10^{-13}$ cm^2 is a more realistic approximation;

C_A — Auger coefficient, $C_A = 10^{-31}$ cm^6 s^{-1} [21];

D_P — in-plane diffusion coefficient of holes within the $Si_{1-x}Ge_x$ layer, $D_P = 10$ cm^2 s^{-1};

d — thickness of the n-doped multilayer absorber;

ε_{Si} and ε_{Ge} — indirect fundamental band gaps of the strained Ge and Si, $\varepsilon_{Si} = 1.12$ eV;

ε_1 and ε_2 — offsets in the conduction and valence bands at the heterojunction between the Si and the $Si_{1-x}Ge_x$ layers, $\varepsilon_2 = 0.1$ eV;

ε_{SG} — band gap of $Si_{1-x}Ge_x$ layer in the spacer, $\varepsilon_2 = \varepsilon_{Si} - \varepsilon_{SG}$;

ε_{Ph} — illumination-induced barrier around the Ge QD, $\varepsilon_{Ph} \approx 0.17$ eV [40];

ε_Γ and ε_V — band gaps between the confined state and the Γ valley in the conduction band, and between the confined state and the Γ valley in the valence continuum band, $\varepsilon_\Gamma = 0.87$ eV [37], $\varepsilon_V = 0.43$ eV;

g_1, g_2, g_{Si} and $g_{\Gamma V}$ integral intensities of infrared photons in the $\varepsilon_V < \hbar\omega < \varepsilon_\Gamma + \varepsilon_V$, $\varepsilon_V < \hbar\omega < \varepsilon_\Gamma$, $\varepsilon_{Si} < \hbar\omega < \varepsilon_\Gamma + \varepsilon_V$ and $\varepsilon_\Gamma + \varepsilon_V < \hbar\omega$ regions of the solar spectrum, $g_1 = g_2 = 1.05 \times 10^{17}$ cm^{-2} s^{-1}, $g_{Si} = 0.42 \times 10^{17}$ cm^{-2} s^{-1} and $g_{\Gamma V} = 1.95 \times 10^{17}$ cm^{-2} s^{-1} [22];

G intensity of the net electron transitions from the valence band into the conduction band via the confined electronic state in the QDs;

j_C and j_V intensities of irradiation-induced transitions from the confined electronic state into the conduction band and from the valence band into the confined electronic state in the QDs

j_{RC} and j_{RV} increase in the intensity of recombination per QD from the conduction band into the confined state, and from the confined state into the valence continuum band;

j_T total photocurrent generated in the Ge QD buried Si solar cell, $j_T \approx 47.5$ A cm^{-2} at the concentration of $S_X = 10^3$;

j_{Si} total photocurrent generated in the conventional Si solar cells, $j_{Si} \approx 38$ A cm^{-2} [22] at the concentration of $S_X = 10^3$;

L distance between buried contacts shown in figure 2, $L = 10$ μm;

L symmetry point of the Brillouin zone;

Γ symmetry point in the centre of the Brillouin zone;

Δ symmetry line of the Brillouin zone;

$\Delta 2$ and $\Delta 4$ valleys on the Δ symmetry line of the Brillouin zone in the conduction band;

m_Γ electron mass in the Γ valley in the conduction band of the bulk Ge, $m_\Gamma = 0.041 m_o$ [37];

n ideality factor of the p–n junctions;

N_D volume density of the Ge QDs, $N_D = 2 \times 10^{16}$ cm^{-3} [5];

$N_{C\Gamma}$ effective number of oscillators involved in the direct transitions in the bulk Ge, $N_{C\Gamma} = 2 \times 10^{17}$ cm^{-3} [37];

N_{SV} density of electronic states in valence band of the $Si_{1-x}Ge_x$ layer, $N_{SV} \approx 2N_V$;

N_V density of states in the valence continuum band of the Ge QDs;

Ω volume of the Ge QD, $\Omega = 10^3$ nm^3 [5, 18];

p_D volume density of confined holes;

p_V density of holes within the $Si_{1-x}Ge_x$ layer of the n-doped $Si/Si_{1-x}Ge_x/Si$ spacer (including photo-generated holes), $p_V \approx \alpha_V (g_2 + g_{\Gamma V}) S_X L^2 / D_P$;

S_X concentration of sunlight, $S_X = 10^3$;

V_{OC} open-circuit voltage induced in the Ge QD buried Si solar cell;

V_{OCSi} open-circuit voltage induced in the conventional Si solar cells;

η conversion efficiency of the Ge QD buried Si solar cell;

η_{Si} conversion efficiency of the conventional Si solar cells, $\eta_{Si} = 37\%$ [22];

τ_1 inter-band recombination lifetime that includes all radiative and non-radiative (and interface) mechanisms for the electron transitions from the conduction band of the $Si/Si_{1-x}Ge_x/Si$ spacer into the confined state in the QD, $\tau_1 = 1$ μs in the type-II Ge QDs buried in the Si matrix [18], $\tau_1 = 1$ μs in the type-II GaSb QDs buried in the GaAs matrix [19];

τ_2 intra-band relaxation lifetime that includes both radiative and non-radiative mechanisms for the electron transitions from the confined state into the valence continuum band in the Ge QD, $\tau_2 = 50$ ps for the intra-band relaxation lifetime [40]

τ_A Auger recombination lifetime given by $\tau_A = 1 / C_A p_V^2$;

z distance from the front-side surface;

ε_Δ energy gap for the direct optical transitions within the $Si/Si_{1-x}Ge_x/Si$ spacer, from the Δ valence band ($E_{V\Delta}$) into the Δ conduction band ($E_{C\Delta}$), $\varepsilon_\Delta = E_{C\Delta} - E_{V\Delta}$;

E_Γ and E_Δ energies of the Γ and Δ bands in the conduction and valence bands;

$E_{\Delta 2}$ and $E_{\Delta 4}$ energies of the spitted Δ bands in the conduction band;

lh and hh light and heavy holes;

1. Introduction

Quantum dots (QDs) [1–7] and wells (QWs) [8, 9] and their integration with the concept of intermediate bands (IBs) [1–3, 10–12] are widely recognized innovative approaches to a higher conversion efficiency solar cell. In the simplest form, the QD solar cell consists of a multilayer of QDs embedded in the built-in electric field of a p–i–n junction. If the material quality is good, the low energy photons generate confined electron–hole pairs in the QDs. Due to the built-in electric field, the generated carriers escape with a high efficiency from the QDs and result in an extra photocurrent. However, like the QW solar cells, the built-in field also increases the generation–recombination current injected from the smaller band gap material, i.e. the QDs, into the semiconductor matrix [5, 8, 9]. Since the generation–recombination current is the dominant component of the dark current in p–n junctions made from wide band gap materials such as Si [13], the increased injection also reduces the conversion efficiency of those solar cells.

The QD solar cells integrated with the concept of IBs [1–3, 10–12, 14, 15] exploit not only the conventional one-photon generation of current but also a generation of an extra photocurrent by the two-photon excitation of electrons from the valence band into the conduction band via the intermediate states embedded within the band gap of an IB absorber [11]. In addition, these solar cells take advantage of the compatibility with high concentrator technology, which reduces the cost of electricity due to substitution of expensive semiconductor

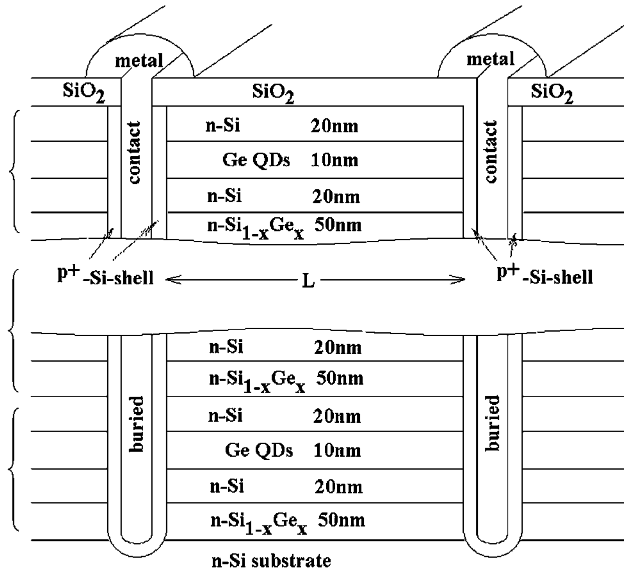

Figure 1. Schematic of the device structures.

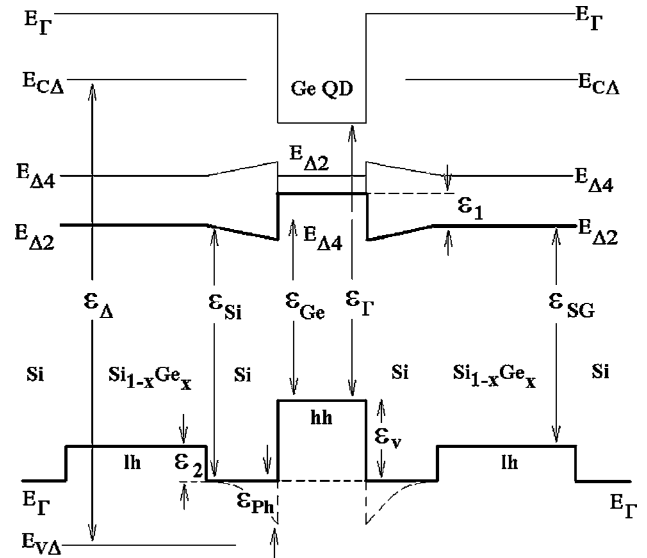

Figure 2. Energy band diagram of the multilayer absorber. ε_Δ is the energy gap for the direct optical transitions within the $Si/Si_{1-x}Ge_x/Si$ spacer, from the Δ valence band ($E_{V\Delta}$) into the Δ conduction band ($E_{C\Delta}$), $\varepsilon_\Delta = E_{C\Delta} - E_{V\Delta}$; E_Γ is the energy of the Γ band in the conduction and valence bands; $E_{\Delta 2}$ and $E_{\Delta 4}$ are the energies of the spitted Δ bands in the conduction band; lh and hh are the light and the heavy holes;

cells with low-cost optics [10, 16]. The conversion efficiency of IB solar cells may exceed the Shockley and Queisser efficiency limit for ideal solar cells and the efficiency of two-terminal tandem cells. Conversion efficiency as high as 63% is expected for ideal IB solar cells [11, 12] where the quasi-Fermi level of the intermediate states is separated from those of the conduction band and the valence band. In fact, the separation of the quasi-Fermi levels is a great problem for energy conversion in IB solar cells [1–3, 11]. Like the electronic states of impurity centres, the intermediate states usually increase the frequency of recombination by arresting quasi-Fermi levels [17]. Evidently, the arresting will be strongly dependent on the energy barrier around QDs. A properly designed barrier can effectively separate the quasi-Fermi levels and suppress the recombination of carriers at the QDs. For instance, a recombination lifetime as long as 1 μs was measured for the inter-band recombination of carriers at QDs with the type II band alignment (GaSb QDs buried in the GaAs matrix and Ge QDs buried in the Si matrix) [18, 19].

In this paper we offer a new structure integrating QDs with the concept of IBs for solar cell applications. The structure has an additional barrier layer built in around Ge QDs buried in a Si-matrix and designed to separate the quasi-Fermi level of the ground confined state from those of the conduction band and the valence band. We analyse the effect of the barrier layer on the photocurrent and on the conversion efficiency of this QD buried solar cell.

2. The model

The structure of the solar cell and the energy band diagram of the QD buried absorber for the Ge/Si material system are schematically shown in figures 1 and 2. The absorber has a multilayer structure, while the QDs have the type-II band alignment. The p–n junctions are formed with the p-doped shells buried deep in the grooves incorporated into the n-doped absorber. The structure shown in figure 1 therefore looks similar to the structure of the buried-contact solar cell [20].

When QDs are at thermal equilibrium, a detailed balance exists among generation–recombination processes and the same Fermi level describes a population of electronic states in all bands and states. However, when the detailed balance is destroyed, e.g., by irradiation-induced additional electron transitions, the Fermi level splits into the quasi-Fermi levels of the conduction band, the valence continuum band and the confined state [11, 12]. Then the equation of continuity, $j_C + j_{RV} = j_V + j_{RC}$, governs the separation of the quasi-Fermi levels and a new occupation of the confined state, p_D, where j_C and j_V are the irradiation-induced electron transitions from the confined electronic state into the conduction band and from the valence band into the confined electronic state in the QD; j_{RV} and j_{RC} are the increase in the intensity of recombination between carriers from the confined state and the valence continuum band, and from the conduction band and the confined state, respectively, [14, 15]. These transitions per QD can be expressed as

$$j_C = \alpha_C g_1 S_X / N_D \tag{1}$$

$$j_V = \alpha_V g_2 S_X / N_D \tag{2}$$

$$j_{RV} = \alpha_V (g_2 + g_{\Gamma V}) S_X (\Omega N_V L^2 / \tau_2 D_P N_{SV}) \times \exp(-(\varepsilon_2 + \varepsilon_{Ph})/kT) \tag{3}$$

$$j_{RC} = p_D / N_D \tau_1. \tag{4}$$

Here α_C and α_V are the absorption coefficients for the direct transitions in the QDs, i.e., from the confined state into the conduction band and from the valence band into the confined state, $\alpha_C = \beta_C (N_D - p_D)$ and $\alpha_V = \beta_V p_D$; β_C and β_V are the relevant absorption cross-sections; S_X is the concentration of the sunlight; N_D is the volume density of the QDs; g_1,

g_2 and $g_{\Gamma V}$ are the integral intensities of infrared photons in the $\varepsilon_\Gamma < \hbar\omega < \varepsilon_\Gamma + \varepsilon_V$, $\varepsilon_V < \hbar\omega < \varepsilon_\Gamma$ and $\varepsilon_\Gamma + \varepsilon_V < \hbar\omega$ ranges of the solar spectrum; ε_Γ is the direct band gap between the confined state and the Γ valley in the conduction band in the Ge QD; ε_V is the band gap between the confined state and the Γ valley in the valence continuum band in the Ge QD; ε_{Ph} is the illumination-induced barrier around the QD; ε_2 is the offset in the valence band at the heterojunction between the Si and the $\text{Si}_{1-x}\text{Ge}_x$ layers shown in figure 2; τ_1 is the inter-band recombination lifetime that includes all radiative and non-radiative (including interface) mechanisms for the electron transitions from the conduction band of the $\text{Si}/\text{Si}_{1-x}\text{Ge}_x/\text{Si}$ spacer into the confined state in the Ge QDs; τ_2 is the intra-band relaxation lifetime that includes both radiative and non-radiative mechanisms for the electron transitions from the confined state into the valence continuum band within the Ge QDs; Ω is the volume of the Ge QD; N_{SV} is the density of electronic states in the valence band of the $\text{Si}_{1-x}\text{Ge}_x$ layer; N_V is the density of states in the valence continuum band of the Ge QD; S_X is the concentration of sunlight; D_P is the in-plane diffusion coefficient of holes within the $\text{Si}_{1-x}\text{Ge}_x$ layer; L is the distance between the buried contacts shown in figure 1.

Equation (3) is derived under the conditions that the distance L is shorter than the in-plane diffusion length of holes within the $\text{Si}_{1-x}\text{Ge}_x$ layer and that the probability of finding an electron in the confined state is greater than the probability of finding a hole in the valence continuum band of the QD,

$$(N_D - p_D)/N_D > p_V \Omega (N_V/N_{\text{SV}}) \exp(-(\varepsilon_2 + \varepsilon_{\text{Ph}})/kT), \tag{5}$$

where p_V is the density of holes in the stack of $\text{Si}_{1-x}\text{Ge}_x$ layers in the roughly $1/\alpha_V$-thick absorber,

$$p_V \approx \alpha_V (g_2 + g_{\Gamma V}) S_X L^2 / D_P. \tag{6}$$

The net generation–recombination transitions from the valence continuum band into the confined state, $j_V - j_{\text{RV}}$, and from the confined state into the conduction band, $j_C - j_{\text{RC}}$, generate mobile electrons and holes within the QDs. For the net transitions to balance each other in the QDs, $j_C - j_{\text{RC}} = j_V - j_{\text{RV}} = G/N_D$, the equation of continuity sets a proper occupation of the confined electronic state p_D and a proper intensity G for the net transitions,

$$p_D = N_D \Bigg/ \left\{ 1 + \frac{1}{\tau_1 g_1 \beta_C S_X} + \frac{g_2 \beta_V}{g_1 \beta_C} \times \left[1 - \left(1 + \frac{g_{\Gamma V}}{g_2} \right) \frac{\Omega N_D N_V L^2}{\tau_2 D_P N_{\text{SV}}} \exp\left(-\frac{\varepsilon_2 + \varepsilon_{\text{Ph}}}{kT} \right) \right] \right\} \tag{7}$$

$$G(z) = -\left[1 - \left(1 + \frac{g_{\Gamma V}}{g_2} \right) \frac{\Omega N_D N_V L^2}{\tau_2 D_P N_{\text{SV}}} \times \exp\left(-\frac{\varepsilon_2 + \varepsilon_{\text{Ph}}}{kT} \right) \right] S_X \frac{\partial g_2}{\partial z}. \tag{8}$$

Equation (8) is derived under the condition that the equations $\partial g_1/\partial z = -\alpha_C(z) g_1(z)$ and $\partial g_2/\partial z = -\alpha_V(z) g_2(z)$ govern the integral intensities of illumination, $g_1(z)$ and $g_2(z)$, where z is the distance from the front-side surface.

If the surface recombination intensity is so weak that approximately all irradiation-induced carriers are collected by p–n junctions in the Ge QD buried Si solar cell, then the two-photon absorption of infrared photons from the $\varepsilon_V < \hbar\omega < \varepsilon_\Gamma + \varepsilon_V$ region of the solar spectrum will generate the photocurrent of $e \int G(z)\,dz$, and the one-photon absorption of photons from the $\varepsilon_\Gamma + \varepsilon_V < \hbar\omega$ region of the solar spectrum will generate the photocurrent of $e S_X g_{\Gamma V}(0)$. We can simplify the integral $e \int G(z)\,dz$ by substituting $g_{\Gamma V}(0)/g_2(0)$ for $g_{\Gamma V}/g_2$ in equation (8). Then, the total photocurrent j_T generated in the Ge QD buried Si solar cell reduces to

$$j_T = e S_X g_2(0) \left[1 - \frac{g_2(d)}{g_2(0)} \right] \left[1 + \frac{g_{\Gamma V}(0)}{g_2(0)} \right] \times \left[1 - \frac{\Omega N_D N_V L^2}{\tau_2 D_P N_{\text{SV}}} \exp\left(-\frac{\varepsilon_2 + \varepsilon_{\text{Ph}}}{kT} \right) \right] \tag{9}$$

where d is the thickness of the multilayer absorber.

The photons from the $\varepsilon_{\text{Si}} < \hbar\omega < \varepsilon_\Gamma + \varepsilon_V$ and $\varepsilon_\Gamma + \varepsilon_V < \hbar\omega$ regions of the solar spectrum will generate the photocurrent of j_{Si} in the conventional Si solar cells,

$$j_{\text{Si}} = e S_X [g_{\text{Si}}(0) + g_{\Gamma V}(0)]. \tag{10}$$

If the Ge QD buried Si solar cell has the same quality p–n junctions with the same dark current, the same ideality factor n and the same fill factor FF as the conventional Si solar cells, then the open-circuit voltage V_{OC} induced in the Ge QD buried Si solar cell will be approximately the same as that V_{OCSi} induced in the conventional Si solar cells, $V_{\text{OC}} = V_{\text{OCSi}} + nkT \times \ln(j_T/j_{\text{Si}})$, while the conversion efficiency η will increase, $\eta = \eta_{\text{Si}} \times (j_T/j_{\text{Si}})$, compared to the efficiency η_{Si} of the conventional Si solar cells. Substituting j_T and j_{Si} in η gives

$$\eta = \eta_{\text{Si}} \times \left[1 + \frac{g_2(0) - g_{\text{Si}}(0)}{g_{\text{Si}}(0) + g_{\Gamma V}(0)} \right] \left[1 - \frac{g_2(d)}{g_2(0)} \right] \times \left[1 - \frac{\Omega N_D N_V L^2}{\tau_2 D_P N_{\text{SV}}} \exp\left(-\frac{\varepsilon_2 + \varepsilon_{\text{Ph}}}{kT} \right) \right]. \tag{11}$$

Under concentrated light irradiation, the Auger recombination lifetime, τ_A, provides an intrinsic constraint upon the recombination lifetime, the open-circuit voltage and the efficiency of Si solar cells, $\tau_A = 1/C_A p_V^2$, where C_A is the Auger coefficient [21]. The same is expected for the recombination lifetime between the electrons and the holes in the $\text{Si}_{1-x}\text{Ge}_x$ layers. Substituting p_V in τ_A therefore gives the following condition for the Auger limit of the efficient charge collection by the $\text{Si}_{1-x}\text{Ge}_x$ layer in the QD buried absorber,

$$S_X (g_2 + g_{\Gamma V}) \alpha_V L^3 \sqrt{C_A / D_P^3} < 1. \tag{12}$$

It is evident that the most intense net generation G and the most separation of the quasi-Fermi levels occur when the irradiation-induced electron transitions are more intense than the relaxations in the QDs. Substituting the generation and the recombination intensities into $j_C > j_{\text{RC}}$ and $j_V > j_{\text{RV}}$ gives the following conditions for the splitting of the Fermi level:

$$\tau_1 g_1 > 1/S_X \beta_C \tag{13}$$

$$g_2 \tau_2 \exp\left(\frac{\varepsilon_2 + \varepsilon_{\text{Ph}}}{kT} \right) > \frac{(g_2 + g_{\Gamma V}) \Omega N_D N_V L^2}{D_P N_{\text{SV}}}. \tag{14}$$

The absorption coefficients of infrared photons are functions of the distance from the front-side surface z of the QD buried absorber. However, under the conditions of (13) and (14), the dependences of α_C and α_V on z disappear if $g_1(0) = g_2(0)$. This gives $g_1(z) = g_2(z)$ and the following results for the most effective conversion:

$$p_D = N_D \beta_C / (\beta_C + \beta_V) \quad (15)$$

$$\alpha_C = \alpha_V = \beta_C \beta_V N_D / (\beta_C + \beta_V) \quad (16)$$

$$G = \alpha_V g_2(0) S_X \exp(-\alpha_V z) \quad (17)$$

$$\frac{\eta - \eta_{Si}}{\eta_{Si}} = \frac{g_2(0) - g_{Si}(0)}{g_{Si}(0) + g_{\Gamma V}(0)}. \quad (18)$$

The density of photon flux in the solar spectrum is approximately 2.5×10^{17} cm^{-2} s^{-1} eV^{-1} in the range of 0.6 eV $< \hbar\omega <$ 1.5 eV [22]. The condition $g_1(0) = g_2(0)$ also yields

$$\varepsilon_\Gamma = 2\varepsilon_V. \quad (19)$$

3. Results and discussion

3.1. Device structure

The absorber shown in figure 1 is a multilayer QD-structure. The Si/Si$_{1-x}$Ge$_x$/Si three-layer heterostructures act as spacers between the approximately 10 nm thick Ge QD-layers. Each spacer consists of a 50 nm thick n-type doped layer of Si$_{1-x}$Ge$_x$ alloy (x $\approx$ 0.2) built in between two 20 nm thick n-type doped Si barrier layers. About 50 layers of these spacers make up an approximately 5 μm thick n-type doped multilayer absorber. A similar stack of $N_D = 2 \times 10^{16}$ cm^{-3} Ge QDs has been grown recently [5]. The stack was composed of 50 QD-layers with about 2×10^{11} cm^{-2} Ge QDs per layer buried in a Si matrix and separated from each other by 40 nm thick Si spacers [5].

Numerous studies have reported on the formation of QD multilayer structures in the Ge/Si material system by MBE and MOCVD using the Stranski–Krastanow growth mode [5, 23–27]. This growth mode was successfully used for tailoring the energy bands [28–34] and the potential barriers around QDs so that mobile electrons of the conduction band can be separated from the confined holes in a real space [18]. For the absorber shown in figure 1 the Si barrier layers act as a wide-band shell-barrier around Ge QDs. The amount of Ge in Si$_{1-x}$Ge$_x$ alloy determines the energy band offset and the height of this shell-barrier ε_2 at the Si/Si$_{1-x}$Ge$_x$ interface in the spacer. The thickness of the Si layer and the amount of Ge in Si$_{1-x}$Ge$_x$ alloy are variable parameters controlled during the growth. Due to these parameters the structure can be tuned within relatively wide margins, which gives a potentially higher flexibility to design and more alternatives to solar cell application of QDs.

3.2. Energy bands

The energy band profile of strained nanostructures is essentially dependent on the residual interfacial strain. The strain lifts the six-fold degeneracy of the conduction band in Δ valleys of the Brillouin zone into Δ2 and Δ4 valleys. These valleys shift in opposite directions by way of constituting the lower conduction band edge. The Δ2 valley constitutes the conduction band minimum in the tensile strained Si spacer, while the Δ4 valley constitutes the conduction band minimum in the Ge QDs since the compressive strain pushes up the L valley and switching the minimum from the L valley to the Δ4 valley in Ge QDs [29–31].

As the Γ point in the centre of the Brillouin zone constitutes a 3.4 eV wide direct band gap in Si and a 0.8 eV wide direct band gap in Ge [31], the potential energy profiles of Γ valleys shown in figure 2 exhibit large discontinuities over the Ge/Si interface in the conduction and valence bands and the type-I alignment over the Ge/Si interface. Even under strain, the conduction band minimum at the Δ4 valley is lower than at the Γ valley. The fundamental band gaps, ε_{Si} and ε_{Ge}, therefore remain indirect in the strained Ge QDs and in the strained Si-layers. Moreover, they acquire real-space indirect character at the interface [34, 35], dramatically reducing the oscillator strength for the radiative inter-band recombination of carriers at the Ge QDs buried in the Si matrix [36].

The strain also lifts the degeneracy between heavy and light holes at Γ valleys in the valence band. The confinement potential picks off a few electronic states from the valance continuum band edge at the Γ valley in the centre of the Brillouin zone and confines them within QDs. Instead, the retained electronic states of the Γ valley constitute a new continuum band edge in the valence band of the Ge QDs below the confinement potential and merge the new edge with the valence band edge of the Si spacer. The new band edges again constitute a direct gap between the Γ valleys in Ge QDs. This direct band gap, as shown in figure 2, is increased up to $\varepsilon_\Gamma + \varepsilon_V$ in Ge QDs, where ε_Γ and ε_V are the gaps between the confined state and the Γ valleys in the conduction and valence continuum bands, respectively. The confinement increases both direct ε_Γ and indirect ε_{Ge} band gaps between the confined state and the conduction band by the energy of confinement.

3.3. Direct optical transitions

Due to the direct optical transitions, the QD multilayer absorber must strongly absorb photons with the integral intensities of g_1, g_2 and $g_{\Gamma V}$ from the $\varepsilon_\Gamma < \hbar\omega < \varepsilon_\Gamma + \varepsilon_V$, $\varepsilon_V < \hbar\omega < \varepsilon_\Gamma$ and $\varepsilon_\Gamma + \varepsilon_V < \hbar\omega$ regions of the solar spectrum. The density of photon flux in the solar spectrum is approximately 2.5×10^{17} cm^{-2} s^{-1} eV^{-1} in the range of 0.6 eV $< \hbar\omega <$ 1.5 eV [22], therefore, the condition $g_1(0) = g_2(0)$ yields $\varepsilon_\Gamma = 2\varepsilon_V$. If $\varepsilon_\Gamma = 0.87$ eV as reported in [37], then equation (19) yields $\varepsilon_V = 0.43$ eV for the optimal energy gap between the valence continuous band and the confined state. For $\varepsilon_\Gamma = 0.87$ eV and $\varepsilon_V = 0.43$ eV, the infrared photons have integral intensities of $g_1 = g_2 = 1.05 \times 10^{17}$ cm^{-2} s^{-1} and $g_{\Gamma V} = 1.95 \times 10^{17}$ cm^{-2} s^{-1} in the solar spectrum [22]. Photons from the spectral region of $\hbar\omega > 2.3$ eV directly transfer electrons from the valence band into the conduction band and generate mobile electrons and holes within an approximately 1 μm thick stack of the Si/Si$_{1-x}$Ge$_x$/Si spacers since the absorption coefficient is as large as 10^4 cm^{-1} in this spectral region in Si.

The confinement potential and the interfacial strain increase the direct energy band between Γ valleys from 0.8 eV up to $\varepsilon_\Gamma + \varepsilon_V = 1.3$ eV [26, 37] in Ge QDs buried in the Si matrix. The photons from the spectral region of $\varepsilon_\Gamma + \varepsilon_V < \hbar\omega$ therefore directly generate mobile electrons and holes within the conduction and valence continuum bands in the Ge QDs. For these direct optical transitions between the Γ valleys, the absorption coefficients α_Γ are expected to be the same in the Ge QDs and in the bulk Ge, $\alpha_\Gamma \geqslant 5 \times 10^3$ cm^{-1}.

Since the confined state of the Ge QDs is at the Γ point in the centre of the Brillouin zone, two consecutive absorptions of the infrared photons from the spectral regions of $\varepsilon_\Gamma < \hbar\omega < \varepsilon_\Gamma + \varepsilon_V$ and $\varepsilon_V < \hbar\omega < \varepsilon_\Gamma$ directly transfer electrons from the confined state into the Γ valley of the conduction band and from the Γ valley of the valence continuum band into the confined state. This two-photon transition generates mobile carriers that diffuse off from the approximately 3 nm thick Ge QD layers in a few femtoseconds. The carriers enter the n-doped $Si/Si_{1-x}Ge_x/Si$ spacer and relax there in picoseconds, e.g., due to the emission of optical phonons. The electron relaxes from the Γ valley into the Δ2 valley of the conduction band, while the hole relaxes from the Si barrier layer into the n-doped $Si_{1-x}Ge_x$ layer of the spacer. The barrier ε_2 in the valence band of the n-doped $Si/Si_{1-x}Ge_x/Si$ spacer separates mobile holes from the confined electronic states of the QDs in real-space, and prevents mobile holes from both radiative and non-radiative transitions back into the QDs.

The absorption coefficients for the direct optical transitions α_C and α_V are proportional to the occupations of the confined state in the Ge QDs, $\alpha_C = \beta_C(N_D - p_D)$ and $\alpha_V = \beta_V p_D$. The cross-sections β_C and β_V are proportional to the relevant oscillator strengths [1, 38] and can be roughly appraised from the absorption coefficient α_Γ and the effective number of oscillators $N_{C\Gamma}$ involved in the direct-transitions in the bulk Ge, $\alpha_\Gamma \approx \beta_\Gamma N_{C\Gamma}$. The effective number of oscillators is approximately equal to the density of states in the Γ valley of the conduction band, where $m_\Gamma = 0.041 m_o$ and $N_{C\Gamma} = 2 \times 10^{17}$ cm^{-3} [37]; therefore the effective cross-section β_Γ for the bulk Ge must be about $\beta_\Gamma \approx 2.5 \times 10^{-14}$ cm^2. The absorption cross-sections are also proportional to the dipole transition matrix elements. Since the overlapping of the envelop functions is stronger in QDs, larger cross-sections are expected for the QDs, $\beta_C > \beta_\Gamma$ and $\beta_V > \beta_\Gamma$.

Measurements performed in the waveguide geometry revealed the inter-band absorption coefficient of 1000 cm^{-1} per 23 nm thick layer of Ge QDs buried in the Si matrix [39]. An absorption cross-section of $\beta_C \approx 8 \times 10^{-13}$ cm^2 can be deduced from these experiments. This result is 30 times larger than $\beta_\Gamma = 2.5 \times 10^{-14}$ cm^2. A photoinduced spectroscopy technique used to measure the intra-band absorption cross-section β_V has revealed the experimental value of $\beta_V = 2 \times 10^{-13}$ cm^2 for Ge QDs buried in the Si matrix [26]. This result is about ten times stronger than β_Γ. The large measured values of absorption cross-sections demonstrate that Ge QDs buried in the Si matrix are very promising for IB solar cells and infrared application.

The discrepancy between the estimated β_Γ and the measured values of the absorption cross-sections β_C and β_V of Ge QDs is too large. This is likely related to a probable quantitative overestimation of the absorption coefficient in the waveguide geometry experiments, which may originate from the weak confinement of the waveguide and the uncertainty on the overlap factor between the guided optical modes and the QD layers [39]. A more realistic approximation for the absorption cross-sections in the Ge QDs is $\beta_{C,V} = 10^{-13}$ cm^2. This value also reflects the large absorption cross-sections measured in experiments.

3.4. Two-photon transitions

The two-photon transition is proportional to the intensity of illumination and to the recombination lifetime. Either the intensity or the lifetime must be so large that, after the first photon-induced electron excitation from the valence band into the confined state, the electron has a large probability for the second photon-induced excitation from the confined state into the conduction band. Since the large recombination lifetime means a large separation of the relevant quasi-Fermi levels, the conditions in equations (13) and (14) for the separation of the quasi-Fermi levels show how large must be the product of the intensity and the lifetime. Evidently, the concentration of light S_X and the special indirect-band separation of the carriers in real-space will support the splitting of the relevant quasi-Fermi levels.

Equation (13) gives the condition for the quasi-Fermi level of the confined state split off from the conduction band. Due to the type-II band alignment, indirect real-space separation prevents the conduction band electrons from recombination with the holes confined in QDs [18, 19]. The inter-band recombination lifetime in equation (13), τ_1, includes all radiative and non-radiative (including interface) mechanisms for the electron transitions from the conduction band of the $Si/Si_{1-x}Ge_x/Si$ spacer into the confined state in the Ge QD. The experimentally determined value of τ_1 is as long as 1 μs for the inter-band recombination of mobile electrons with confined holes in the type-II Ge QDs buried in the Si matrix [18] and the type-II GaSb QDs buried in the GaAs matrix [19]. Also the inter-band recombination from the conduction band into the valence band of the indirect band-gap $Si/Si_{1-x}Ge_x/Si$ spacer is about 1 μs [18]. It is not yet completely clear how the real-space indirect-band separation in the conduction band suppresses inter-band recombination of mobile electrons with confined holes in the type-II QDs. Nevertheless, the suppression makes it possible to liberate the quasi-Fermi level of mobile carriers from that of the confined state. Substituting the numerical values of parameters $\beta_C \approx 10^{-13}$ cm^2, $g_1(0) = 1.05 \times 10^{17}$ cm^{-2} s^{-1} and $\tau_1 = 1$ μs into equation (13) reveals that the concentration of $S_X = 10^3$ is enough for the strong separation of the quasi-Fermi levels in the conduction band and the activation of the electron transitions from the confined state into the conduction band in the Ge QD buried Si solar cell.

Equation (14) gives the condition for the quasi-Fermi level of the confined state split off from the continuum valence band. Since holes are the minority carriers in the n-type doped absorber, the condition in equation (14) is independent of the concentration of sunlight S_X. The intra-band relaxation lifetime τ_2 includes both radiative and non-radiative transitions of electrons from the confined state into the valence continuum band within the Ge QDs. The mid-IR pump–probe experiments on Ge QDs buried in a Si matrix revealed $\tau_2 = 50$ ps for the intra-band relaxation lifetime [40]. The 'phonon bottleneck' effect and the acoustic phonon emission are responsible for the long intra-band-relaxation lifetime [40]. The barrier ε_2 in the valence band of the n-doped $Si/Si_{1-x}Ge_x/Si$ spacer shown in figure 2 separates the illumination-induced mobile holes from the electrons excited into the confined state. The holes diffuse the distance L along the $Si_{1-x}Ge_x$ layer, rather than overwhelm the barrier height ε_2

in the valence band and recombine with the confined electrons or diffuse perpendicular to the stack of the $Si/Si_{1-x}Ge_x/Si$ spacers. Therefore the real-space separation of carriers exponentially increases the recombination lifetime and the two-photon absorption cross-section in the Ge QDs.

Electrons completely occupy the confined electronic state at thermal equilibrium, $p_D = 0$. Under illumination, however, the two-photon transitions insert holes into the confined electronic state, $p_D > 0$. These holes transfer a positive charge into the QDs and induce a barrier ε_{Ph} around the Ge QDs [40]. Calculation showed that the induced barrier may be as large as $\varepsilon_{Ph} \approx 0.17$ eV [40]. Also this irradiation-induced barrier ε_{Ph} will separate mobile holes from the confined electronic states in real-space and prevent mobile holes from transitioning back into the QDs.

Substituting the following numerical values for parameters $N_D = 2 \times 10^{16}$ cm^{-3} [5], $N_{SV} \approx 2N_V$, $\tau_2 = 50$ ps [40], $D_P = 10$ cm^2 s^{-1}, $g_r(0)/g_2(0) \approx 2$, $\Omega = 10^3$ nm^3 [5, 18], $\varepsilon_{Ph} \approx 0.1$ eV and $L = 10$ μm into equation (14) reveals that an energy barrier as high as $\varepsilon_2 = 0.1$ eV is enough for the strong separation of the quasi-Fermi levels in the valence band and the activation of the electron transitions from the valence continuum band into the confined state in the Ge QD buried Si solar cell.

Equation (12) refers to the Auger limit on the recombination lifetime in the Ge QD buried Si solar cell. Evidently, the diffusion of holes along the $Si_{1-x}Ge_x$ layers towards p–n junctions must be faster than the Auger recombination with electrons. Substituting the following numerical values $D_P = 10$ cm^2 s^{-1}, $C_A = 10^{-31}$ cm^6 s^{-1} [21], $g_2 + g_{\Gamma V} = 3 \times 10^{17}$ cm^{-2} s^{-1}, $\alpha_V = 5 \times 10^3$ cm^{-1} and $L = 10$ μm into equation (11) yields the Auger limit on the concentration of light, $S_X < 10^4$.

The continuity of the electron transitions introduces a correlation between the absorption coefficients α_C and α_V, and makes them dependent on the distance z and on the ratio between the integral intensities of illumination g_1/g_2. Under the conditions (13), (14) and $g_1(0) = g_2(0)$, however, according to equation (16), the dependence on z disappears in the absorption coefficients and the net transitions yield $G = \alpha_C g_1 S_X = \alpha_V g_2 S_X$. Substituting the following numerical values $\beta_C = \beta_V \approx 10^{-13}$ cm^2 and $N_D = 2 \times 10^{16}$ cm^{-3} into equation (16) gives $\alpha_C = \alpha_V \approx 10^3$ cm^{-1} for the two-photon absorption.

3.5. Conversion efficiency

The continuity of the electron transitions through the confined state results in an occupation of the confined state such that the net transitions $j_C - j_{RC}$ and $j_V - j_{RV}$ balance each other everywhere within the multilayer absorber. Equation (7) predicts that the balanced occupation is strongly dependent on the barrier $\varepsilon_2 + \varepsilon_{Ph}$ around the QDs. This strong dependence also transfers into equations (9) and (11) of the photocurrent j_T and the conversion efficiency η.

Figure 3 exhibits the dependence of η on the barrier height $\varepsilon_2 + \varepsilon_{Ph}$ for the following numerical values of parameters: $\Omega = 10^3$ nm^3 [5, 18], $N_{SV} \approx 2N_V$, $N_D = 2 \times 10^{16}$ cm^{-3} [5], $g_{Si} = 0.42 \times 10^{17}$ cm^{-2} s^{-1}, $g_2(0) = 1.05 \times 10^{17}$ cm^{-2} s^{-1}, $g_{\Gamma V} = 1.95 \times 10^{17}$ cm^{-2} s^{-1}, $D_P = 10$ cm^2 s^{-1}, $L = 10$ μm, $\tau_2 = 50$ ps [40], $g_2(d) = 0$, $\eta_{Si} = 37\%$ [22] and $S_X = 10^3$. As shown in figure 3, the conversion efficiency η grows exponentially with barrier height. The saturation about $\eta = 46.5\%$ occurs when the barrier in the valence band is as high as $\varepsilon_2 + \varepsilon_{Ph} = 0.2$ eV. When $\varepsilon_2 + \varepsilon_{Ph} < 0.12$ eV, the conversion efficiency of the Ge QD buried Si solar cell drops below that of the conventional Si solar cell, since the condition in equation (14) is never met and the QDs come to act as active recombination centres. Conditions (13) and (14) are also relevant to the electronic states of recombination centres in doped and compound semiconductors. For instance, the abrupt decrease in the performance of GaInNAs solar cells with the addition of nitrogen, as noted in [17], indicates a fast relaxation of carriers and an arrest of the electron quasi-Fermi level by the nitrogen traps.

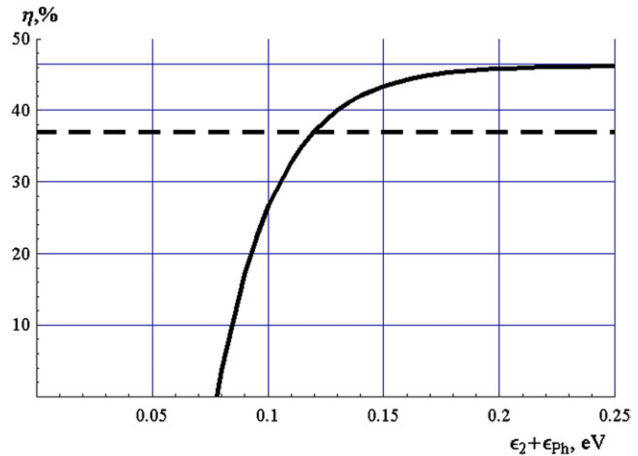

Figure 3. Conversion efficiency η as a function of the barrier $\varepsilon_2 + \varepsilon_{Ph}$ in the valence band. Solid line—the Ge QD buried Si solar cell; dashed line—the conventional Si solar cell, $\eta_{Si} = 37\%$.

Equations (9) and (10) give $j_T \approx 47.5$ A cm^{-2} for the photocurrent induced in the Ge QD buried Si solar cell at the concentration of $S_X = 10^3$, and $j_{Si} \approx 38$ A cm^{-2} [22] for the photocurrent induced in the conventional Si solar cell. The enhanced photocurrent increases the conversion efficiency of the optimized Ge QD buried Si solar cell nearly 25% in comparison to the conventional Si solar cell. In particular, the conversion efficiency limit for the ideal one p–n junction Si solar cell shown in figure 3 will increase from 37% [22] to 46% in the optimized Ge QD buried Si solar cell.

4. Conclusion

In summary, a model of the QD buried solar cells is described. The main difference from the other models is that a barrier layer is built in around QDs in the spacer. The conditions in which the quasi-Fermi level of confined carriers splits from the quasi-Fermi levels of mobile carriers were found and expressed with equations (13) and (14). It was shown quantitatively that the separation of the quasi-Fermi levels is strongly dependent on the barrier height and that the barrier can strongly resist arresting the quasi-Fermi level at the confined state. This study of the Ge/Si material system showed that a barrier as low as $\varepsilon_2 = 0.1$ eV in the valence band can increase the short-circuit current and the conversion efficiency of the Ge

QD buried Si solar cell by 25%, as compared to the same quality conventional Si solar cells.

Acknowledgments

This work was supported by the National Science Council of Taiwan under grant no NSC 95-2112-M-009-046 and partly supported by the Armenian Ministry of Education and Science under grant no 0441-136-01.02.2005.

References

[1] Cuadra L, Martí A, Lopez N and Luque A 2004 A phonon bottleneck effect and photon absorption in self-ordered quantum dot intermediate band solar cells *19th European Photovoltaic Solar Energy Conf. and Exhibition (Paris, France, 7–11 June)*

[2] Martí A, Cuadra L and Luque A 1999 Quantum dot super solar cell *Proc. Conf. Sobre Dispositivos Electrónicos (Madrid, Spain)* pp 363–6

[3] Martí A, Cuadra L and Luque A 2000 Quantum dot intermediate band solar cell *Proc. 28th IEEE Photovoltaic Specialist Conf. (Fairbanks, AK)*

[4] Nozik A J 2002 Quantum dot solar cells *Physica* E **14** 115

[5] Konle J, Presting H and Kibbel H 2003 Self-assembled Ge-islands for photovoltaic applications *Physica* E **16** 596

[6] Aroutiounian V, Petrosyan S, Khachatryan A and Touryan K 2001 Quantum dot solar cells *J. Appl. Phys.* **89** 2268

[7] Aroutiounian V, Petrosyan S and Khachatryan A 2005 Studies of the photocurrent in quantum dot solar cells by the application of a new theoretical model *Sol. Energy Mater. Sol. Cells* **89** 165

[8] Barnham K *et al* 1996 Voltage enhancement in quantum well solar cells *J. Appl. Phys.* **80** 1201–6

[9] Nelson J, Ballard I, Barnham K, Connolly J P, Roberts J S and Pate M 1999 Effect of quantum well location on single quantum well p-i-n photodiode dark currents *J. Appl. Phys.* **86** 5898

[10] Sala G 2005 PV concentration in Spain: technology and market perspectives *Taiwan Symp. on HCPV Systems (INER, Taiwan, 15 Nov.)*

[11] Luque A and Marti A 1997 Increasing the efficiency of ideal solar cells by photon induced transitions at intermediate levels *Phys. Rev. Lett.* **78** 5014

[12] Luque A, Marty A, Stanley C, Lopez N, Cuadra L, Zhou D, Pearson J L and McKee A 2004 General equivalent circuit for intermediate band devices: potentials, currents and electroluminescence *J. Appl. Phys.* **96** 903–8

[13] Pikus G E 1965 *Theory of Semiconductor Devices* (Moscow: Nauka)

[14] Kechiantz A M, Sun K W, Kechiyants H M and Kocharyan L M 2005 Self-ordered Ge/Si quantum dot intermediate band photovoltaic solar cells *Int. Sci. J. Altern. Energy Ecol.* **12** 85–7

[15] Kechiantz A M, Sun K W, Kechiyants H M and Kocharyan L M 2005 Suppression of dark current in two-step photovoltaic cells *Proc. 5th Int Conf. on Semiconductor Micro- and Nano-Electronics (Aghveran, Armenia, 16–18 Sept.)* p 235

[16] Araki K, Uozumi H, Egami T, Hiramatsu M, Miyazaki Y, Kemmoku Y, Akisawa A, Ekins-Daukes N J, Lee H S and Yamaguchi M 2005 Development of concentrator modules with dome-shaped Fresnel lenses and triple-junction concentrator cells *Prog. Photovolt. Res. Appl.* **13** 513–27

[17] Kurtz S, Johnston S and Branz H M 2005 Capacitance-spectroscopy identification of a key defect in N-degraded GaInNAs solar cells *Appl. Phys. Lett.* **86** 113506

[18] Fukatsu S, Sunamura H, Shiraki Y and Komiyama S 1997 Phononless radiative recombination of indirect excitons in a Si/Ge type-II quantum dot *Appl. Phys. Lett.* **71** 258

[19] Hatami F *et al* 1998 Carrier dynamics in type-II GaSb/GaAs quantum dot *Phys. Rev.* B **57** 4635–41

[20] Green M A 1998 *Solar Cells in Modern Semiconductor Device Physics* ed S M Sze (New York: Wiley)

[21] Green M 1984 Limits on the open-circuit voltage and efficiency of silicon solar cells imposed by intrinsic Auger processes *IEEE Trans. Electron Devices* **31** 671

[22] Sze S M 1981 *Physics of Semiconductor Devices* (NewYork: Wiley)

[23] Chang W-H, Chen W-Y, Chou A-T, Hsu T-M, Chen P-S, Pei Z and Lai L-S 2003 Effects of spacer thickness on optical properties of stacked Ge/Si quantum dots grown by chemical vapor deposition *J. Appl. Phys.* **93** 4999–5002

[24] Bao Y, Liu W L, Shamsa M, Alim K, Balandin A A and Liu J L 2005 Electrical and thermal conductivity of Ge/Si quantum dot superlattices *J. Electrochem. Soc.* **152** G432

[25] Schmidt O G and Eberl K 2000 Multiple layers of self-asssembled Ge/Si islands: photoluminescence, strain fields, material interdiffusion, and island formation *Phys. Rev.* B **61** 13721–9

[26] Boucaud P, Le Thanh V, Sauvage S, Debarre D and Bouchier D 1999 Intraband absorption in Ge/Si self-assembled quantum dots *Appl. Phys. Lett.* **74** 401–3

[27] Tong S, Liu, Khitun A, Wang K L and Liu J L 2004 Tunable normal incidence Ge quantum dot midinfrared detectors *Appl. Phys. Lett.* **96** 773–6

[28] Shchukin V A and Bimberg D 1999 Spontaneous ordering of nanostructures on crystal surfaces *Rev. Mod. Phys.* **71** 1125

[29] Schmidt O G, Eberl K and Rau Y 2000 Strain and band-edge alignment in single and multiple layers of self-assembled Ge/Si and GeSi/Si islands *Phys. Rev.* B **62** 16715–20

[30] El Kurdi M, Sauvage S, Fishman G and Boucaud P 2006 Band-edge alignment of SiGe/Si quantum wells and SiGe/Si self-assembled islands *Phys. Rev.* B **73** 195327

[31] Schaffler F 1997 High-mobility Si and Ge structures *Semicond. Sci. Technol.* **12** 1515–49

[32] Liu C W, Maikap S and Yu C-Y 2005 Mobility-enhancement technologies *IEEE Circuits Devices Mag.* May/June 21–36

[33] Lee M L, Fitzgerald E A, Bulsara M T, Currie M T and Lochtefeld A 2005 Strained Si, SiGe, and Ge channels for high-mobility metal–oxide–semiconductor field-effect transistors *J. Appl. Phys.* **97** 011101

[34] Sfina N, Lazzari J-L, Derrien J, d'Avitaya F A and Said M 2005 Strain-balanced $Si_{1-x}Ge_x$/Si type II quantum wells for 1.55 μm detection and emission *Eur. Phys. J.* B **48** 151–6

[35] Dashiell M W, Denker U and Schmidt O G 2001 Photoluminescence investigation of phononless radiative recombination and thermal-stability of germanium hut clusters on silicon(001) *Appl. Phys. Lett.* **79** 2261

[36] Laheld U E H, Pedersen F B and Hemmer P C 1995 Excitons in type-II quantum dots: finite offsets *Phys. Rev.* B **52** 2697

[37] Kou Y-H, Lee Y K, Ge Y, Ren S, Roth J E, Kamins T I, Miller D A B and Harris J S 2005 Strong quantum-confined Stark effect in germanium quantum-well structures on silicon *Nature* **437** 1334–6

[38] Huag H and Koch S W 1993 *Quantum Theory of the Optical and Electronic Properties of Semiconductors* (Singapore: World Scientific)

[39] Elkurdi M, Boucaud P, Sauvage S, Kermarrec O, Campidelli Y, Bensahel D, Saint-Girons G and Sagnes I 2002 Near-infrared waveguide photodetector with Ge/Si self-assembled quantum dots *Appl. Phys. Lett.* **80** 509–11

[40] Halsall M P, Dunbar A D F, Shiraki Y, Miura M and Wells J-P R 2004 Hole confinement and dynamics in δ-doped Ge quantum dots *J. Luminescence* **108** 329–32